



Mesomechanics 2009

## Delamination analysis of holed composite laminates using interface elements

H. Hosseini-Toudeshky<sup>a,\*</sup>, M. Jalalvand<sup>a</sup>, B. Mohammadi<sup>a</sup>

<sup>a</sup>*Aerospace engineering department & Center of excellence in computational aerospace engineering  
Amirkabir University of Technology, Tehran, Iran*

Received 1 March 2009; revised 21 April 2009; accepted 24 April 2009

---

### Abstract

In this paper interface element with de-cohesive constitutive law is used to predict the failure load of laminates containing a central hole in which delamination is the dominant failure mode of them. For this purpose, the initiation and propagation of inter-laminar crack are modeled using our in house FEM code. It is shown that at a certain load step, the interface elements between the two layers of  $-45^\circ$  and  $0^\circ$  fail abruptly. It is also shown that the predicted failure stresses of laminates with various thicknesses are in an acceptable agreement with the experimental results.

Keywords: delamination, interface element, composite, hole, lamianate

---

### 1. Introduction

Failure analysis of laminated composites is generally complex due to diverse mechanisms that may arise. The damage can be divided into two categories of in-plane or intra-laminar failure (e.g. fiber fracture or inter-fiber fracture like transverse matrix cracking, fiber–matrix debonding etc.), and delamination or inter-laminar failure. Geometrical discontinuities, such as holes, cut-outs, free edges, stiffener terminations, ply drop-offs, or bonded and bolted joints can provoke both intra- and inter-laminar failure due to the high stress gradients arising. The presence of lay-up mismatch can also increase inter-laminar stresses at the mentioned locations. Therefore, delamination is one of the most likely and common types of failure mode in laminated composites due to their weak inter-laminar strength.

Delamination analysis is normally performed to predict the delamination initiation or propagation. For determining the onset of inter-laminar cracks, stress-based criteria such as proposed in [1] can be applied to investigate the edge delamination. Delamination propagation analyses are mainly based on the existence of an initial crack by the application of the fracture mechanics theory in which fracture parameters such as stress intensity factor and energy release rate may be used to check whether the crack propagates or not .

---

\* Corresponding author. Tel.: +98-21-6454-3224; fax: +98-21-66959020.  
E-mail address: [hosseini@aut.ac.ir](mailto:hosseini@aut.ac.ir).

An alternative method capable of predicting both initiation and propagation of delamination is the use of the damage zone concept. The use of meso-modeling in the analysis of composite delamination has been firstly proposed by Ladevez et al. [2-5]. In this type of modeling, the composite laminate is conceived as an assemblage of two main constituents: the fiber-reinforced layer and the separation interface which is called damage zone here. The attribution to these of an interface constitutive law allows the modeling of delamination i.e. progressive loss of cohesion between the adjacent layers [3]. In this approach, the interface is considered as the third independent material entity which links two components and is defined by its own constitutive law [6]. In this method a softening constitutive law is attributed to the damage zone and therefore both damage initiation and propagation can be modeled by a gradual degradation of the interface. Implementing a softening constitutive law into the FEM using interface elements is usually a straightforward task, and constitutes one of the main advantages of this method compared with the FEM fracture mechanics [7].

In spite of the abundant literature on the subject, the choice of proper interface models and the identification of their parameters are critical issues [6]. The elastic-plastic-damage constitutive model proposed in [3] is used in the current investigation. There exist many more constitutive models presented in the literature not discussed here due to the limited space. In spite of such variety of constitutive laws, in most cases, a unique interface identification process could be performed using the knowledge of the matrix yield point or the lateral strength of the composite layer, and the energy release rate in three directions.

The dominant failure mode of composite laminates is strongly related to the stacking sequence of the layers [8], material properties, and the geometry of the specimens. Green and Wisnom performed an extensive experimental investigation of the scale effects on notched composites and described how the dimensions of a specimen can affect the failure mechanism [9]. They compared the experimental failure loads with the Average Stress Criterion (ASC) predictions. They found that, when the damage mechanism is brittle fracture or fiber pull-out, ASC results are acceptable, but, that the criterion fails in the case of delamination. In this paper, the failure loads of the specimens subjected to the delamination as dominant failure mechanism are carried out.

## 2. Constitutive Law

Plastic deformation and damage parameter vectors are two variables determining the nonlinear state. Equation (1) describes the variation of an inter-laminar stress component with respect to nonlinear state variables.

$$d\tau_i = K_i(1 - \varphi_i)du_i^e - u_i^e K_i d\varphi_i. \quad (1)$$

Here  $\tau_i$ ,  $K_i$ ,  $\varphi_i$  and  $u_i^e$  ( $i=1, 2, 3$ ) are stress, interface penalty stiffness, damage parameter and elastic displacement discontinuity components of each three inter-laminar directions respectively. The yield surface, which determines the limits of elastic or elastic-plastic-damage behavior, is presented by equation (2). The equation is similar to the classic quadratic initiation criterion used to determine the initiation of inter-laminar crack, where the effective stress values of undamaged state are substituted.

$$F(\tau_i, \varphi_i) = \sqrt{a_1 \left( \frac{\tau_1}{1 - \varphi_1} \right)^2 + a_2 \left( \frac{\tau_2}{1 - \varphi_2} \right)^2 + a_3 \left( \frac{\langle \tau_3 \rangle^+}{1 - \varphi_3} \right)^2} - 1 - h(\lambda) = 0 \quad \& \langle \tau_3 \rangle^+ = \begin{cases} \tau_3 & \text{if } \tau_3 > 0 \\ 0 & \text{if } \tau_3 \leq 0 \end{cases} \quad (2)$$

Here  $\lambda$  is the plastic-damage multiplier which governs the magnitude of plastic deformation and damage variables, and  $h(\lambda)$  describes the softening rule, and here  $h(\lambda) = -\lambda$ . When the stress at a certain point reaches the yield surface and its direction is outward,  $\lambda$  is increased from its initial value of zero. While  $\lambda$  is increased,  $1 - \lambda$  is decreased causing the shrinkage of yield surface indicating the softening behaviour of the material in the damage zone.  $a_i$  ( $i=1, 2, 3$ ) are material constants obtained from matrix yield point. To avoid penetration of coincident faces and considering the closure effect in the direction 3 or opening mode, an exceptional condition was applied in this direction and the positive quantities of normal inter-laminar stresses are only considered to be effective in terms of damage and plasticity development. The variation of plastic displacement discontinuity and damage parameters are governed by the flow rule and evolution law and have been assumed in the manner in [3] and will not be stated here due to the space limitation.

### 3. Analyses of Notched Specimens

Three different quasi-isotropic laminates of  $[45_m/90_m/-45_m/0_m]_S$  ( $m=1, 2$  or  $4$ ) containing holes with diameter of 3.175mm were considered. Within all specimens the ratios of width and length to hole diameter were constant  $W/d=5$  and  $L/d=20$ . The specimens are selected by the criterion that their dominant failure mode is delamination, as determined by the experiments. The material is IM7/8552, a unidirectional carbon-fiber/epoxy with ply thickness of 0.125mm, with mechanical properties of:  $E_{11}=161\text{GPa}$ ,  $E_{22}=E_{33}=11.38\text{GPa}$ ,  $\nu_{12}=\nu_{13}=0.32$ ,  $\nu_{23}=0.45$ ,  $G_{12}=G_{13}=5.17\text{GPa}$ ,  $G_{23}=3.92\text{GPa}$  and the  $G_C$  is  $380\text{ J/m}^2$  from [10]. Fig. 1(a) shows the geometry, loading and mesh of a typical specimen. Due to the symmetry of the lay-ups, half of the laminates are modeled in the Z direction. Since it is explicitly mentioned in [9] that the delamination initiates at the interface of  $-45/0$  plies and covers the whole of the laminate at this interface, the cohesive zone or the interface elements are considered at the mentioned location and the adjacent plies ( $-45^\circ$  and  $0^\circ$ ) are meshed with three 20-noded brick elements in the Z direction as shown in Fig. 1(b). In mesh convergence study, it became clear that three elements in the Z direction are necessary to obtain acceptable inter-laminar stresses at the interface. On the other hand, the applied constitutive law for the damage zone includes softening and it may cause convergence difficulties. The specimen is not symmetrical in the width direction and the damage will initiate and propagate from both sides of the hole in the width direction. Therefore, to decrease the computational time, half of the model is meshed by the coarse elements and the other side is meshed with the fine elements as indicated in Fig. 1(d). By this kind of modeling, we will focus on the fine mesh for damage initiation and propagation. Elastic and elastic-plastic-damage analyses of the specimens were performed using our software (AUTDMA-IF85) [11]. Fig. 2 compares the obtained inter-laminar elastic stresses at the interface of  $-45/0$  around the quarter of the hole for two different meshes applying the remote strain of 0.2%. This figure shows that the obtained stresses at  $\theta=60^\circ$  (especially  $\tau_{xz}$ ) are more critical than the other positions indicating that the damage may initiate from this location. Details of the used cohesive law diagram are available in [3] and are not depicted here due to the space limitation.

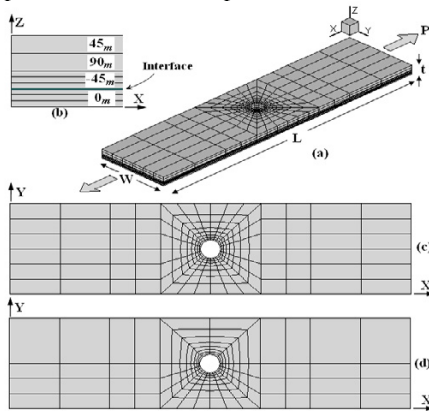


Fig. 1. Mesh, (a) 3D view of specimen, (b) mesh in thickness direction, (c) mesh1, (d) mesh2

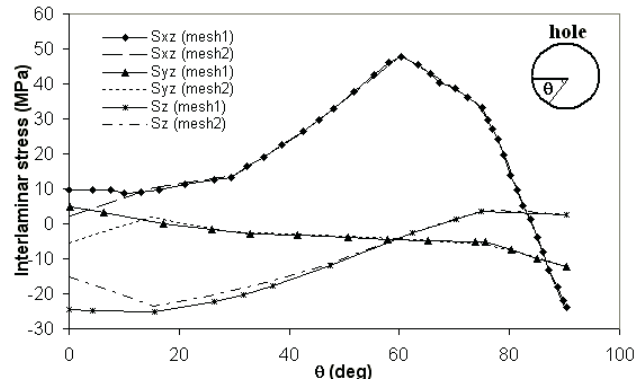


Fig. 2. Comparison of inter-laminar stresses at  $-45/0$  interface along the circumference of the hole for mesh1 and mesh2

Displacement control loading is applied to all specimens by an incremental procedure. At certain load step, it was observed that applying a small load increment caused a global unstable behavior. At this load step all interface elements were damaged, i.e. the solution diverges and this load step can be considered to correspond to the catastrophic inter-laminar crack growth or unstable delamination propagation. Fig. 3 shows the distribution of the damage parameter at the interface around the hole in the final load increment and different iterations before the final failure. The predicted failure loads of various specimens are compared with those obtained from the experiments [9] in Table 1. This table shows that the differences between the predicted failure load using the present study and those obtained from the experiments are 6.5% for  $[45_2/90_2/-45_2/0_2]_S$  lay-up and it is conservative, 5.4% for  $[45_4/90_4/-45_4/0_4]_S$  lay-up, and 14.8% for  $[45_8/90_8/-45_8/0_8]_S$  lay-up. Both experimental and numerical results show that the

failure stresses of the laminates are decreased by increasing the thickness of the laminates. The obtained failure stress reduction rate with respect to the laminate thickness from this study is smaller than that found in the experimental results which may be due to the existence of other type of damages that have not been taken into account in this study.

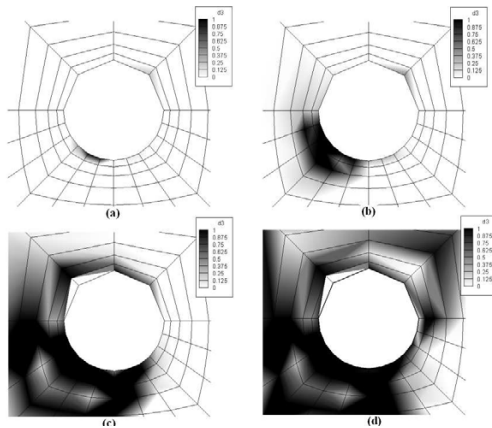


Figure 3. Damage at interface elements around the hole (a-d) damage at final load step and different iterations

#### 4. Conclusion

Using interface elements with cohesive constitutive law, failure load of laminates by delamination as the dominant failure mode was predicted. For this purpose, the initiation and propagation of inter-laminar crack was modeled. It was observed that at certain load step the interface elements between the layers of  $-45^\circ$  and  $0^\circ$  were abruptly destroyed and this phenomenon occurred along with the increase of damage parameters in the damage zone. It was also shown that the predicted failure stresses of laminates with various thicknesses follows a trend that agrees with the experimental results.

#### References

1. C.T. Sun, S.G. Zhou. Failure of quasi-isotropic composite laminates with free edges. *J Reinforced Plastics and Composites* 1988;7:515-557
2. P.Ladeveze. A damage mechanics for composite materials. *Integration of Theory and Application in Applied Mechanics* 1990;13-24
3. A. Corigliano. Formulation, identification and use of interface models in the numerical analysis of composite delamination. *J of Solid Structures* 1993;30:20:2779-2811
4. O. Allix, P. Ladeveze. Inter-laminar interface modeling for the prediction of delamination. *J Composite Structure* 1992;22: 235-242
5. O. Allix, P. Ladeveze, A. Corigliano. Damage analysis of inter-laminar fracture specimens. *J Composite Structure* 1995;31:61-74
6. A. Corigliano, O.Allix. Some aspects of inter-laminar degradation in composites. *Comput Methods App. Mech Eng* 2000;185:203-224
7. Z. Zou, S.R. Reid,S. Li. A continuum damage model for delaminations in laminated composites. *J of the Mechanics and Physics of Solids* 2003;51:333-356.
8. N.J. Pagano, R.B. Pipes.The influence of stacking sequence on laminate strength. *J Composite Materials* 1971;5:50-57
9. B.G. Green, M.R. Wisnom, S.R. Hallett. An experimental investigation into the tensile strength scaling of notched composites. *Composites Part: A* 2007;38:867-878
10. R. Krueger, J. G. Ratcliffe, P.J. Minguet. Panel stiffener debonding analysis using a shell/3D modeling technique *Compos Sci Technol* (2009), doi:10.1016/j.compscitech.2008.12.015
11. H. Hosseini-Toudeshky, M. Jalalvand, B. Mohamadi. Delamination of laminates governed by free edge inter-laminar stresses using interface element. *Key Eng Material* 2008;385-387:821-824

Table 1. Failure load of different specimens and comparison of the obtained results and available experimental data

No.	Laminate	Hole diameter (mm)	Present Study	Exp. [9]
			$\sigma_x$ (MPa)	$\sigma_x$ (MPa)
1	[45 <sub>2</sub> /90 <sub>2</sub> /-45 <sub>2</sub> /0 <sub>2</sub> ] <sub>S</sub>	3.175	370	396
2	[45 <sub>4</sub> /90 <sub>4</sub> /-45 <sub>4</sub> /0 <sub>4</sub> ] <sub>S</sub>	3.175	290	275
3	[45 <sub>8</sub> /90 <sub>8</sub> /-45 <sub>8</sub> /0 <sub>8</sub> ] <sub>S</sub>	3.175	232	202